Deficiency of cyclin-dependent kinase-like 5 causes spontaneous epileptic seizures in neonatal mice

Wenlin Liao[1,2] *, Kun-Ze Lee[3], Jinchung Chen[4], San-Hua Su[1,5] and Yuju Luo[1]

[1] Institute of Neuroscience, National Cheng-Chi University, Taipei 116, Taiwan

[2] Research Center for Mind, Brain and Learning, National Cheng-Chi University, Taipei 116, Taiwan

[3] Department of Biological Sciences, National Sun Yat-sen University, Kaohsiung 804, Taiwan

[4] Graduate Institute of Biomedical Sciences, Chang Gung University, Taoyuan 333, Taiwan

[5] Department of Chinese Medicine, Buddhist Tzu Chi General Hospital, Hualien 970, Taiwan (Present address)

---

* To whom correspondence should be addressed:

Wenlin Liao, PhD

Associate Professor
Institute of Neuroscience, National Cheng-Chi University
64, Sec. 2, Chi-Nan Road, Wen-Shan District
Taipei 116, Taiwan

Phone: 886-2-29393091 ext. 89621
Email: wlliao@nccu.edu.tw

Abstract

Cyclin-dependent kinase-like 5 (*CDKL5*), an X-linked gene encoding a serine-threonine kinase, is enriched in the mammalian forebrain and critical for neuronal maturation and synaptic function. Mutations in this gene cause CDKL5 deficiency disorder (CDD), which is characterized by early-onset epileptic seizures, motor dysfunction and intellectual disability. Although several mouse models for CDD have been developed, overt spontaneous seizures have not been reported in adult mice with CDKL5 deficiency. Here, we present the first systematic study of spontaneous seizures in a mouse model of CDD. Through wireless electroencephalography (EEG) recording in a longitudinal manner, we observed epileptiform discharges in pups lacking CDKL5. The total number of spike events, the total burst number and burst duration were significantly increased in *Cdkl5* null pups at the age of postnatal day 12 (P12). With age, these seizure-like discharges gradually diminished in mutant pups, while the discharges increased progressively in wild-type mice. Through simultaneous videotaping, *Cdkl5* null pups exhibited seizure-like behaviors during prolonged bursts of discharges at P12, and showed increased ictal grasping and grip strength in adults. Notably, loss of CDKL5 remarkably down-regulated the phosphorylation of K^+-Cl^- co-transporter 2 (KCC2) in the cortex and hippocampus at P12. Our findings reveal a previously unidentified age-dependent phenotype of early-onset seizures in CDKL5-deficient neonatal mice, enhancing the translational value of CDD mouse model and providing a potential molecular target for early diagnosis and therapeutic development for CDD.

Introduction

CDKL5 deficiency disorder (CDD; OMIM#300672; ICD-10-CM code: G40.42) is a developmental and epileptic encephalopathy caused by mutations in the X-linked gene encoding cyclin-dependent kinase-like 5 (CDKL5; OMIM#300203). This disorder is characterized by severe early onset seizures, autistic features, and intellectual disability (Archer et al 2006, Scala et al 2005, Weaving et al 2004), and categorized as one of the most common forms of genetic epilepsy (Lindy et al 2018, Symonds et al 2019). The epileptic activities accompanied with developmental delays in children with CDD are frequently associated with devastating cognitive, psychiatric and behavioral disabilities later in life. Elimination of early-onset epilepsy may potentially ameliorate the consequent developmental delays of this disorder (Demarest et al 2019, Fehr et al 2016, Scheffer et al 2017). Despite well-defined genetic cause, however, children with CDD are resistant to most of the anti-epileptic drugs (AEDs) and the pathogenic mechanisms for CDKL5 deficiency-induced seizures remain unclear.

Several mouse models of CDD have been developed that display behavioral phenotypes mimicking primary symptoms of CDD, but intriguingly, spontaneous seizures have not been reported (Amendola et al 2014, Jhang et al 2017, Okuda et al 2018, Wang et al 2012). In the study of first mouse model, normal basal electroencephalographic (EEG) patterns and powered frequency distributions in the hippocampus were recorded using deep electrodes for up to 240 hours in *Cdkl5* null mice carrying a complete deletion of exon 6 (Wang et al 2012). Upon kainic acid administration, mice lacking *Cdkl5* exon 4 show epileptiform of events but normal basal EEG was recorded at least in the somatosensory cortex (Amendola et al 2014). In addition, spontaneous seizures have not been found in the third CDD mouse model with *Cdkl5* deletion of exon 2, even though mutant mice exhibited enhanced seizure susceptibility in response to NMDA treatment (Okuda et al 2017). Notably, all the behavioral observations and EEG recordings for seizure activities in these studies were conducted in adult mice aged from 1 to 4 months. Considering that the median age of seizure onset in CDD patients is about 6 weeks after birth and that a "honeymoon period" with seizure cessation can last up to 72 months (Bahi-Buisson et al 2008, Fehr et al 2016), it is possible that early onset of spontaneous seizures were missed in those studies of adult mice.

Empirically, when we performed ultrasound vocalization recordings during postnatal day 4 (P4) to P10, we noticed that *Cdkl5* knockout (exon 6 deletion, *Cdkl5*$^{-/y}$) pups showed increased spasm-like twists compared to wild-type (WT) pups (Jhang et al 2017)(Liao, unpublished observations). The spasm-like behaviors have been observed in mice with *Arx* gene mutations that cause infantile spasm (Marsh et al 2009, Price et al 2009). We reasoned that pups lacking CDKL5 might experience early-onset seizures during the early stage after birth. However, EEG recordings and seizure behaviors have not been reported and measured in pre-weaning pups with CDKL5 deficiency, we thus carried out longitudinal EEG recordings with miniature wireless transmitters coupled with simultaneous videotaping in mouse pups at the first three weeks of age. To reveal possible molecular targets for therapeutic development, the protein expression affected by CDKL5 deficiency in neonatal mice was also investigated.

Results

Wireless EEG recording in mouse pups

To identify potential EEG abnormalities in *Cdkl5*$^{-/y}$ mice, we implanted a transmitter onto pups at P10, the youngest age possible for this experiment, and accessed the EEG activity using a miniature telemetry system (Fig. 1) (Zayachkivsky et al 2013). Data collected by transmitters that were damaged in the following days (2 in 12), likely gnawed by the dam, were excluded from analysis. Compared with the WT littermate controls, abnormal seizure-like discharges were observed in *Cdkl5*$^{-/y}$ pups starting from P11, one day after the transmitter was implanted (Fig. 1C, Fig. 2).

Increased seizure-like discharges in *Cdkl5*$^{-/y}$ pups

Given that the battery power of the transmitters can last up to 14 days, we collected EEG data from P11 to P24 upon implantation at P10. The EEG recordings demonstrated that the population spikes tended to increase in WT but decrease in *Cdkl5*$^{-/y}$ pups with age (Fig. 2). Notably, loss of CDKL5 apparently increased EEG activity in pups during the P11-14 period (Fig. 2A-C'), whereas fewer discharges were found in *Cdkl5*$^{-/y}$ pups at P24 compared to WT pups (Fig. 2F, F'). The latter observation was consistent with previous reports in which adult *Cdkl5* null mice lack spontaneous seizures (Amendola et al 2014, Okuda et al 2017, Wang et al 2012). Further analysis of the EEG activities at P12 revealed that epileptiform discharges occurred in *Cdkl5*$^{-/y}$ pups repeatedly in the episodes of 10-20 sec (Fig. 3B', C'). These episodes were not detected in WT littermate control pups (Fig. 3B, C).

Loss of CDKL5 triggers spontaneous seizures at P12

To quantify the electrographic spikes, we processed the EEG traces of the last 90 min in each day of the recording (i.e., 10-100 min) using Clampex software. For event detection, the "threshold" amplitude was set to 0.9 volts based on the pilot tests (arrow and dash line in Fig. 4A). We found that the total number of events was altered between genotypes with age [interaction of genotype x age: $p = 0.0003$, $F(5, 36) = 6.265$], in which it was significantly higher in *Cdkl5*$^{-/y}$ pups compared to that in WT pups at P12 (3766 ± 961.7 in KO vs. 410.3 ± 118.6 in WT, $p < 0.001$; Fig. 4B, C; Suppl. Table 1). To compare the amplitude of spike events, the output spikes of 1V was equivalent to 0.25 mV for the original intensity due to 4000x amplification by the transmitters. The result showed that the mean event amplitude was comparable between genotypes with age, although there was a trend of increase observed at P11 and P12 (Fig. 4D, E; Suppl. Table 1). In addition, there was no significant alteration in the mean frequency of total events in *Cdkl5*$^{-/y}$ pups compared to WT pups with age, except a slight increase found in *Cdkl5*$^{-/y}$ pups at P12 (Fig. 4F, G; Suppl. Table 1).

We next evaluated the seizure-like activities through a burst analysis, in which a "burst" was defined as a series of continuous discharges for more than 20 events whose inter-event-intervals were less than 1 sec. The "total number of bursts" was increased in *Cdkl5*$^{-/y}$ compared to WT pups at P12, however, the burst number became comparable between genotypes from P14 to P24, demonstrating possible normalization of EEG

activities in *Cdkl5*$^{-/y}$ pups with age (Fig. 5A, B; Suppl. Table 1). Notably, the "duration of bursts" and the "number of events per burst", both indicating the severity of seizure-like discharges, were significantly increased in *Cdkl5*$^{-/y}$ pups compared to WT littermates at P12 ($p < 0.001$; Fig. 5C-F; Suppl. Table 1). The enhancement subsided and returned to WT levels during the following days. The frequency of events in burst, though, did not change in CDKL5-deficient pups compared to WT littermates through P11 to P24 (Fig. 5G, H; Suppl. Table 1).

Increased spasm-like movements in bursting *Cdkl5*$^{-/y}$ pups

Given that behavioral seizures have been observed as a primary outcome of neonatal epilepsy (Aujla et al 2009, Marsh et al 2009, Price et al 2009), we next analyzed the videos captured simultaneously with EEG recordings to identify potential behavioral seizures that occurred during the electrographic events of bursts. We selectively reviewed the behaviors of pups at P12 that happened during the prolonged bursts extending longer than the mean duration of bursts. We found frequent twitches of limbs, tail flicks, occasional jerky movements of the body and rapid stretching of limbs during the prolonged bursts in *Cdkl5*$^{-/y}$ pups (Fig. 6A, upper panels; Suppl. Movie#1), while WT littermate pups tended to rest quietly without obvious movements during the bursting period (lower panels in Fig. 6A; Suppl. Movie#2). Following quantification of these spasm-like behaviors by scoring them from 0 to 3, we found that the accumulative scores were consistently higher in *Cdkl5*$^{-/y}$ pups compared to the scores derived from the WT littermate pups (Fig. 6B).

Enhanced ictal grasping in *Cdkl5*$^{-/y}$ mice

Given that "ictal grasping" has been identified in patients with frontal hyperkinetic seizures, which presents increased grasping forces after the seizure onset (Gardella et al 2006, Leiguarda et al 2008), we next measured the grasping activities in pups of WT and *Cdkl5* mutants using the wire suspension test. From P14, the mutant pups tended to grasp the wire for a longer time than their WT littermate pups did, and then the holding time of mutant pups increased significantly at P18 (46.1 ± 7.2 sec in KO vs. 19.8 ± 2.1 sec in WT, $p < 0.001$; Fig. 6C). This result suggests that, in addition to triggering onset of seizures at P12, loss of CDKL5 also enhances ictal grasping later in life, at least at the pre-weaning age in mice.

To clarify if the enhancement of ictal grasping persists to adulthood, we next examined grip strength of these mice at the age of 4-6 weeks. By pulling the tails of the tested mice with a steady force, the peak force of their forelimbs grasping a T-shaped bar can be measured. The results showed that the rate of pulling force (i.e., slope of peak force) was comparable between groups, suggesting that the force we applied to pull the tails was smooth and steady (212.04 ± 8.27 in KO vs. 190.59 ± 14.55 in WT, $p > 0.05$; Fig. 6D). As increased grasping in the pre-weaning age, *Cdkl5*$^{-/y}$ young adults exhibited increased grip strength (peak force, gF) per gram of body weight (gF/g: 5.45 ± 0.15 in KO vs. 4.14 ± 0.29 in WT, $p < 0.001$; Fig. 6E) as well as prolonged holding time of grasping compared to their littermate controls (0.74 ± 0.02 sec in KO vs. 0.67 ± 0.01 sec in WT, $p < 0.01$; Fig. 6F). These traits persisted with age, as similar grip enhancement

was found in mutants at 5-7 months of age (gF/g: 9.33 ± 0.37 in KO vs. 5.84 ± 0.29 in WT, $p < 0.001$; Fig. 6E). Of note, the implanted *Cdkl5*$^{-/y}$ pups exhibited an increase of ~1.8-fold in locomotor activities at P31 compared to their WT littermates in an open field test (Traveled distance: 5683.5 ± 450.7 cm in KO vs. 3222.1 ± 206.4 cm in WT, $p < 0.001$; Fig. 6G), suggesting that the neonatal implantation of transmitters and the longitudinal EEG recordings during early postnatal age did not attenuate the behavioral phenotype of hyperlocomotion in *Cdkl5*$^{-/y}$ mice (Jhang et al 2017, Wang et al 2012).

Reduced functional K-Cl co-transporter KCC2 in *Cdkl5*$^{-/y}$ cortex at P12

CDKL5 has been reported to translocate into the nucleus by P14 and may regulate gene expression by phosphorylation of transcriptional regulators (Rusconi et al 2008). The developmental induction of the neuronal K^+/Cl^- co-transporter 2 (KCC2), which extrudes intracellular chloride anions, has been reported to be essential to the ontogenetic switch of $GABA_A$-mediated responses from depolarizing to hyperpolarizing (Rivera et al 1999). The expression and function of KCC2 is thus a key to control neuronal excitability in neonates, and KCC2 dysfunction has been implicated in pathogenesis of infantile epilepsy (Moore et al 2017, Puskarjov et al 2014). Notably, phosphorylation of KCC2 at the residue of serine 940 (pKCC2-S940) is crucial for stabilizing KCC2 on the surface of neuronal membrane that enables extrusion of Cl^- (Lee et al 2007). Given our findings of age-dependent epileptic activities in *Cdkl5*$^{-/y}$ pups, it raises a possibility that CDKL5 deficiency affects the protein expression and phosphorylation of KCC2 in the cortical neurons at P12.

We therefore measured the phosphorylation status and protein expression level of KCC2 by immunoblotting in cortical tissue of mice with and without CDKL5. We found that loss of CDKL5 significantly reduced the phosphorylation level of pKCC2-S940 as well as the proportion of pKCC2-S940 in total KCC2 compared to that in WT littermate pups (0.58 ± 0.056 of WT, $p < 0.01$; Fig. 7A, B). By contrast, phosphorylated KCC2 at threonine 1007 (pKCC2-T1007), which inhibits transport function (Inoue et al 2012), was not changed in *Cdkl5*$^{-/y}$ pups (0.913 ± 0.071 of WT, $p > 0.05$; Fig. 7A, C). The alterations of phosphorylated KCC2 were recapitulated in the hippocampus of CDKL5-deficient pups at P12 (data not shown). In addition to unaltered expression of total KCC2 (1.005 ± 0.070 of WT, $p > 0.05$; Fig. 7A, D), the expression of developmentally down-regulated cation-chloride co-transporter, Na+-K+-Cl- co-transporter 1 (NKCC1) that drives transport of Cl^- into the cells (Yamada et al 2004), remained unchanged in CDKL5-deficient pups (0.953 ± 0.041 of WT, $p > 0.05$; Fig. 7A, E).

In terms of the proteins related to excitation/ inhibition (E/I) balance, we found normal expression of $GABA_A$ receptors (0.991 ± 0.025 of WT, $p > 0.05$; Fig. 7A, F), GABA synthesizing enzyme glutamate decarboxylase 2 (GAD2; 1.063 ± 0.011 of WT, $p > 0.05$; n = 3) and vesicular GABA transporter (vGAT; 1.017 ± 0.026 of WT, $p > 0.05$; n = 3) for the inhibitory transmission in cortical tissues of *Cdkl5*$^{-/y}$ pups. The protein levels of vesicular glutamate transporter 2 (vGluT2; 0.983 ± 0.027 of WT, $p > 0.05$; n = 3) and cannabinoid receptor 1 (CB1R; 0.937 ± 0.071 of WT, $p > 0.05$; n = 3), the excitatory presynaptic markers, were also unchanged with CDKL5 deficiency. However, the protein level of PSD-95, a CDKL5-interacting protein in the postsynaptic density of

excitatory synapses, was reduced in pups lacking CDKL5 (0.812 ± 0.049 of WT, $p < 0.01$; Fig. 7A, G, consistent to previous findings in adult mutants or in cultured neurons (Della Sala et al 2016, Lupori et al 2019, Pizzo et al 2016, Ricciardi et al 2012, Zhu et al 2013).

Discussion

In the present study, we longitudinally measured EEG in neonatal mice using wireless setup and videotaped their behaviors in parallel, and then quantified EEG discharges and bursts from P11 to 24. We found that pups with CDKL5 deficiency exhibited increased epileptiform discharges selectively at P12, with drastic increase of the total number of spike events, the total number of bursts, the mean duration of bursts and the mean event number per burst compared to WT littermate controls. These mutant pups also showed seizure-like behaviors, such as limb stretch, tail flicks and jerky body movement, during bursting period at P12. Enhanced ictal grasping, manifested in *Cdkl5* mutant pups at late pre-weaning stage, was sustained to adults shown as increased grip strength and holding duration. Notably, loss of CDKL5 significantly decreased the phosphorylation level of pKCC2-S940 and reduced the proportion of functional KCC2 in the developing cortex. Our findings suggested that loss of CDKL5 increases susceptibility for epileptic activities in neonatal mice at P12, possibly associated with neuronal hyper-excitability caused by anomalously prolonged GABA-mediated excitation.

As a mouse model of CDD, *Cdkl5*$^{-/y}$ mice have exhibited numerous behavioral phenotypes recapitulating features in CDD (Amendola et al 2014, Jhang et al 2017, Mazziotti et al 2017, Okuda et al 2018, Wang et al 2012). Intriguingly, early-onset epilepsy, the symbolic trait in children with CDD, has not been reported in previous studies. Given that eighty percent of children with CDD have daily seizures, and the epileptic spasms onset at a median age of 6 weeks followed by a seizure-free honeymoon period (Demarest et al 2019, Fehr et al 2016, Olson et al 2019), we reasoned that onset of epilepsy in mice with CDKL5 deficiency might occur at around neonatal age and alleviate later in life. By using a miniature telemetry system for wireless EEG recording in mouse pups, here, we identified robust epileptiform discharges in pups with CDKL5 deficiency selectively at P12. We noticed a trend of increase in total number of both events and bursts in WT pups from P12 to P24 (Fig. 4A and 5A). With increased activities in WT pups, the EEG profiles in *Cdkl5*$^{-/y}$ pups appeared slight reduction compared to WT at P24 (Fig. 4C), which is consistent to the previous findings of reduced number of epileptiform events in adult *Cdkl5*$^{-/y}$ mice (Amendola et al 2014). Our results did not exclude the possible occurrence of seizure onset prior to P12 in CDKL5-deficient mice. However, considering the survival rate of pups upon implantation surgery, the wireless EEG recording by the transmitters used in the present study is hardly applied to pups less than 6 g that is about the body weight of mouse pups at P10, making it impossible to record EEG in pups younger than P10.

To elucidate the possible mechanism for the age-dependent early onset seizures, we measured the expression of proteins engaged in the developmental switch of hyperpolarizing GABAergic inhibition, which has been implicated in pathogenesis of neonatal seizures (Moore et al 2017, Puskarjov et al 2014, Rivera et al 1999). We found

that CDKL5 deficiency significantly decreased the cortical expression of pKCC2-S940 by ~40% at P12 (Fig. 7). The KCC2 protein does not express in rat hippocampus until P5 and reaches to the adult level after P10 (by P15) (Rivera et al 1999), which time point is corresponding to P9.1-13.2 in mouse according to the translating developmental time across species (Clancy et al 2001). Our findings that loss of CDKL5 reduced the proportion of functional KCC2 (pKCC2-S940) without altering the expression of total KCC2 suggest that loss of CDKL5 may cause hypofunction of KCC2, which impairs the transition of GABAergic response from excitation to inhibition, leading to seizure onset in *Cdkl5*$^{-/y}$ pups at the neonatal stage. Therefore, CDKL5 plays a key role to maintain KCC2 function and render the initiation of GABAergic inhibition during neonatal stage. Similar with this, reduction of KCC2 and delayed GABA functional switch has been reported in neurons from Rett syndrome (RTT) patients, suggesting the possible existence of a common mechanism for the epileptic trait in CDD and RTT (Kadam et al 2019, Tang et al 2016). The intracellular location of KCC2, the characteristics of KCC2-positive neurons and excitabilities of GABA receptive neurons in neonatal CDKL5-deficient mice should be further verified by anatomical and electrophysiological studies.

On the other hand, given that KCC2 has not been identified as a direct substrate of CDKL5 (Baltussen et al 2018, Munoz et al 2018), the CDKL5-dependent regulation of pKCC2 might be conducted indirectly through the action of protein kinase C, which has been reported to interact with CDKL5 and phosphorylate KCC2 at S940 (Lee et al 2007, Wang et al 2012). Although we did not find alterations in the protein expression of some molecules related to E/I balance (including pKCC2-T1007, NKCC1, GABAA receptor, GAD2, vGAT, vGluT2, CB1R) in the cortex at P12, the possible involvement of other E/I players, such as NMDA receptors, AMPA receptors and pavalbumin, in CDKL5-dependent onset of neonatal seizures could not be excluded (Okuda et al 2017, Pizzo et al 2016, Tang et al 2017, Yennawar et al 2019). Pup EEG recording in different lines of *Cdkl5* mutant mice and further biochemical studies are helpful to reveal the detail mechanisms of CDKL5-dependent early onset seizures.

Although many clinical cases of CDD have present spontaneous grasping of objects at months of age (Bartnik et al 2011), the majority of children with CDD exhibit delayed raking grasp, especially in males (Fehr et al 2015). Our findings of persistent enhancement in grasping duration and strength in both neonatal and adult mice (Fig. 6) suggest that the grasping behavior could be a robust trait representing the behavioral outcome for the hypermotor-tonic-spasms type of epilepsy in the frontocentral region (Gardella et al 2006, Klein et al 2011, Leiguarda et al 2008, Melikishvili et al 2019). In view of the expression of KCC2 in human, it reaches to the equivalent level as that in P10-15 rat at the early infancy stage (Kang et al 2011), which is corresponding to the period of seizure occurrence in children with CDD (Demarest et al 2019, Fehr et al 2016). Our findings of epileptic discharges in *Cdkl5*$^{-/y}$ mouse pups at P12, therefore could be temporally relevant to the time window of seizure onset in children with CDD, in terms of KCC2 expression. Given that children with CDD are often unresponsive to AEDs or responding without long-term efficacy (Dale et al 2019, Muller et al 2016, Olson et al 2019), the KCC2 activators might be an alternative for treating CDD based on our findings. However, no study has reported the perinatal expression of functional KCC2 in children with CDD to date. The detection of functional KCC2 in cases and

pharmacological testing of KCC2 activators in mice might be pilot works to pursue cure for CDD.

Together, in the present study, we identified early-onset seizures, from both EEG and video recordings, in CDKL5-deficient mice, offering construct and face validity for this mouse model of CDD. We also revealed the CDKL5-mediated regulation of functional KCC2, providing a potential biomarker for diagnosis and target for therapeutic development. By leveraging the gestational diagnosis and intervention, an effective remedy for early onset seizures and the consequent developmental delays in children with CDD is in sight.

Materials and Methods

Animals. Male *Cdkl5* null pups were generated by crossing C57BL/6J male mice (National Laboratory Animal Center, Taiwan) to heterozygous *Cdkl5* females [$Cdkl5^{+/-}$, B6.129(FVB)-$Cdkl5^{tm1.1Joez}$/J](Wang et al 2012). Male hemizygous pups ($Cdkl5^{-/y}$) and their littermate controls ($Cdkl5^{+/y}$) were used as the experimental cohorts to avoid mosaic expression of *Cdkl5* due to random X-inactivation. All mice were bred and housed in individually ventilated cages (IVC, Alternative Design, USA) at 22 ± 2°C and 60 ± 10 % humidity under a 12-hour light-dark cycle (light on 08:00 to 20:00). Irradiated diet (#5058, LabDiet, USA) and sterile water were supplied *ad libitum*. All experiments were approved by the Institutional Animal Care and Use Committee at National Cheng-Chi University.

Pup EEG recording - Implantation of transmitters. Male pups were tail-marked and genotyped at P9. Genotyping was performed as previously described (Jhang et al 2017). Only the pups with a body weight of > 6 g were subjected to transmitter implantation. Each pup at P10 was implanted under 1% isoflurane anesthesia in O_2 for ~20 min. The transmitters (4 x 6 mm in size of footprint, 8 mm in height, 0.5 g for each; gain = 4000 x) were activated according to the manufacturer's instructions (Epoch, Epitel, USA) before use, which then kept transmitting EEG activities for two weeks after activation. The bilateral EEG electrodes (2 channels, ~2 mm in between) were cut to ~2-3 mm and then implanted symmetrically to the midline at the middle level of the cortex (Zayachkivsky et al 2013). A reference electrode (~4 mm posterior to channel1) was positioned to the left hemisphere just anterior to the Lambda. The transmitter was secured onto the skull with tissue glue (Vetbond, 3M). After surgery, the implanted pups were kept on a pre-warmed plate until awakening, and then monitored for EEG activity for 20 min to confirm success of implantation. The pups were then returned to their home cage and nurtured by the dam. The body weight and general health of implanted pups were monitored on a daily basis after surgery to confirm their recovery and growth. Six pairs of pups were successfully implanted and survived. Due to unexpected failure of the transmitters during the experiments (P11-24), however, only four pairs (from four litters) of data were available for statistics.

Pup EEG recording - data acquisition and analysis. For longitudinal EEG studies, these pups were placed in a transparent plastic box (10 cm x 10 cm) and recorded daily between 1-6 pm for 100 min in the first four days post-surgery (P11-14), followed by recording at P17, 21, and 24. EEG activities were captured with a receiver (Epoch, Epital) connected to a data acquisition system (PowerLab, ADInstruments) controlled by the LabChart 7 software. The sampling rate was 1000 Hz. The raw data were first processed by digital filter with a cut-off frequency at 50

Hz (low-pass) and 3 Hz (high-pass), and then the traces for period of 10-100 min (90 min) were exported to Clampex (Version 10.7, Axon Instruments) for further analysis. For event detection, the threshold was set as 0.9 V (equivalent to 0.225 mV of input intensity) to detect spike discharges (events). For the burst analysis, a burst was defined as a continuous train of discharges that contains more than 20 spikes with the inter-spike interval of < 1 sec. The measurements for event/burst parameters (duration, frequency, and amplitude) were exported to Excel for statistic analysis. Given that the EEG data of longitudinal recordings containing some missing values, they were analyzed by fitting a mixed model rather than by a repeated measures ANOVA (which cannot perform analysis on data with missing values) (Prism 8, GraphPad).

Assessment for seizure-like behaviors. During the EEG recording, potential seizure-like behaviors were videotaped simultaneously using a webcam (Logitech). The pups' behaviors at P12 selectively derived from the prolonged bursts whose durations were longer than the mean burst duration were evaluated according to a previous report (Price et al., 2009). The behavioral seizures were scored from 0 to 3 with the following criteria: 0, sleeping/ staying quiet without movement; 1, staying quiet with occasional orofacial movement/ head bobbing/ forelimb twitch/ tail flick; 2, freezing suddenly during movement; and 3, spasm-like jerky movements of the head, body or limbs. The additive scores for time-locked spasm-like behaviors during the prolonged bursts for each *Cdkl5*$^{-/y}$ pup were compared to their WT littermates (see Suppl. Movies).

Wire suspension. To test grip strength and endurance, the forepaws of the mouse pups were positioned on a horizontal wire (3 mm in diameter) suspended at a height of 30 cm above the tabletop (Schneider and Przewlocki, 2005). Soft bedding materials were placed under the wire to protect fallen pups from injury. Each pup was tested for five trials every other day from P10 to P18. The latency to fall was recorded with a cutoff time of 3 min for each trial. The median of daily scores for *Cdkl5*$^{-/y}$ pup and their WT littermates was compared by two-way repeated measures ANOVA (Prism 8, GraphPad).

Grip strength measurement. The grip strength was measured by a grip strength meter (UGO Basile, Italy) in adult mice (including the transmitter-implanted mice) during the afternoon hours of the light cycle (2-6 pm). The force transducer was placed at a height of ~2.5 cm from the base plate. The tested mice were pulled against the T-shaped bar for 10 times with an inter-trial interval of 30 seconds to avoid muscle fatigue. The "peak force" (in grams, gF), "peak time" (i.e., the latency time of the animal response), and "total holding duration" were recorded. The rate of applied pulling force (target force rate, slope, i.e., gF/sec) was calculated to confirm the steady force of application. The "force per unit weight" (gF/g), estimated from the mean of 10 trials, was used to compare the grip strength in mice carrying different genotypes.

Immunoblotting. Immunoblotting was performed as previously described (Jhang et al 2017). The cortical and hippocampal tissues were harvested from *Cdkl5*$^{-/y}$ pups and their WT littermates at the age of P12, and then homogenized by sonication in lysis buffer containing 1% protease inhibitors and 1% phosphatase inhibitor (Sigma). Twenty micrograms of protein were separated in 4-15% polyacrylamide gel (Bio-Rad) with 125 V for 100 min. The proteins were transferred to PVDF membranes (Millipore) with 350 mA for 2 h (Mini Trans-Blot Cell, Bio-Rad). The membranes were blocked using 5% skim milk for 1 h and then incubated with primary antibodies against CDKL5 (1:1,000, Abcam), KCC2 (1:1,000, Millipore), pKCC2-S940 (1:5,000, PhosphoSolutions), pKCC2-T1007 (1:5,000, PhosphoSolutions), NKCC1 (1:10,000, Millipore),

PSD-95 (1:2,000, ThermoFisher), $GABA_A$R-gamma 2 (1:2,000, Millipore), GAD2 (1:1,000, Cell Signaling), CB1R (1:5,000, Abcam), VGAT (1:1,000, SYSY), VGLUT2 (1:1,000, SYSY), glyceraldehyde 3-phosphate dehydrogenase (GAPDH, 1:50,000, Millipore) at 4 °C for 16 h. Following incubation with peroxidase-conjugated secondary antibodies at room temperature for 2 h, the target proteins were detected by an enhanced chemoluminescence reagent (ECL, Millipore) with an image acquisition system (Biostep, Germany). After the pKCC2 were detected, the membranes were stripped and re-blocking, followed by incubation of antibodies for KCC2. The intensity of target protein expression was quantified with densitometry (Image J, NIH) and normalized with the loading control of GAPDH. The protein expression in mutants was presented as "ratio to WT" and the Student'*s t*-test was used for comparison.

Acknowledgments

This work is supported by grants from the Ministry of Science and Technology, Taiwan [MOST107-2320-B-004-001-MY3 to WL; MOST108-2636-B-110-001 to KZL] and the International Foundation of CDKL5 Research, USA [2015~2019 to WL].

Conflict of interest

The authors declare no competing financial interests.

Supplementary information

Table 1. Quantification and statistic results for longitudinal measurement of EEG discharges from mouse pups

Movie#1. Representative behavior of a *Cdkl5*$^{-/y}$ pup during a prolonged burst at P12

Movie#2. Representative behavior of a WT pup during a prolonged burst at P12

References

Amendola E, Zhan Y, Mattucci C, Castroflorio E, Calcagno E, et al. 2014. Mapping pathological phenotypes in a mouse model of CDKL5 disorder. *PLoS One* 9: e91613

Archer HL, Evans J, Edwards S, Colley J, Newbury-Ecob R, et al. 2006. CDKL5 mutations cause infantile spasms, early onset seizures, and severe mental retardation in female patients. *J. Med. Genet.* 43: 729-34

Aujla PK, Fetell MR, Jensen FE. 2009. Talampanel suppresses the acute and chronic effects of seizures in a rodent neonatal seizure model. *Epilepsia* 50: 694-701

Bahi-Buisson N, Nectoux J, Rosas-Vargas H, Milh M, Boddaert N, et al. 2008. Key clinical features to identify girls with CDKL5 mutations. *Brain* 131: 2647-61

Baltussen LL, Negraes PD, Silvestre M, Claxton S, Moeskops M, et al. 2018. Chemical genetic identification of CDKL5 substrates reveals its role in neuronal microtubule dynamics. *EMBO J* 37: pii: e99763.

Bartnik M, Derwinska K, Gos M, Obersztyn E, Kolodziejska KE, et al. 2011. Early-onset seizures due to mosaic exonic deletions of CDKL5 in a male and two females. *Genet Med* 13: 447-52

Clancy B, Darlington RB, Finlay BL. 2001. Translating developmental time across mammalian species. *Neuroscience* 105: 7-17

Dale T, Downs J, Olson H, Bergin AM, Smith S, Leonard H. 2019. Cannabis for refractory epilepsy in children: A review focusing on CDKL5 Deficiency Disorder. *Epilepsy Res* 151: 31-39

Della Sala G, Putignano E, Chelini G, Melani R, Calcagno E, et al. 2016. Dendritic Spine Instability in a Mouse Model of CDKL5 Disorder Is Rescued by Insulin-like Growth Factor 1. *Biological psychiatry* 80: 302-11

Demarest ST, Olson HE, Moss A, Pestana-Knight E, Zhang X, et al. 2019. CDKL5 deficiency disorder: Relationship between genotype, epilepsy, cortical visual impairment, and development. *Epilepsia* 60: 1733-42

Fehr S, Downs J, Ho G, de Klerk N, Forbes D, et al. 2016. Functional abilities in children and adults with the CDKL5 disorder. *Am J Med Genet A* 170: 2860-69

Fehr S, Leonard H, Ho G, Williams S, de Klerk N, et al. 2015. There is variability in the attainment of developmental milestones in the CDKL5 disorder. *J Neurodev Disord* 7: 2

Gardella E, Rubboli G, Tassinari CA. 2006. Ictal grasping: prevalence and characteristics in seizures with different semiology. *Epilepsia* 47 Suppl 5: 59-63

Inoue K, Furukawa T, Kumada T, Yamada J, Wang T, et al. 2012. Taurine inhibits K+-Cl- cotransporter KCC2 to regulate embryonic Cl- homeostasis via with-no-lysine (WNK) protein kinase signaling pathway. *J Biol Chem* 287: 20839-50

Jhang CL, Huang TN, Hsueh YP, Liao W. 2017. Mice lacking cyclin-dependent kinase-like 5 manifest autistic and ADHD-like behaviors. *Hum Mol Genet* 26: 3922-34

Kadam SD, Sullivan BJ, Goyal A, Blue ME, Smith-Hicks C. 2019. Rett Syndrome and CDKL5 Deficiency Disorder: From Bench to Clinic. *Int J Mol Sci* 20

Kang HJ, Kawasawa YI, Cheng F, Zhu Y, Xu X, et al. 2011. Spatio-temporal transcriptome of the human brain. *Nature* 478: 483-9

Klein KM, Yendle SC, Harvey AS, Antony JH, Wallace G, et al. 2011. A distinctive seizure type in patients with CDKL5 mutations: Hypermotor-tonic-spasms sequence. *Neurology* 76: 1436-8

Lee HH, Walker JA, Williams JR, Goodier RJ, Payne JA, Moss SJ. 2007. Direct protein kinase C-dependent phosphorylation regulates the cell surface stability and activity of the potassium chloride cotransporter KCC2. *J Biol Chem* 282: 29777-84

Leiguarda RC, Nouzeilles MI, Ugarnes G, Amengual A, Roldan E, et al. 2008. Ictal non-forced grasping behaviour. *Eur J Neurol* 15: 169-72

Lindy AS, Stosser MB, Butler E, Downtain-Pickersgill C, Shanmugham A, et al. 2018. Diagnostic outcomes for genetic testing of 70 genes in 8565 patients with epilepsy and neurodevelopmental disorders. *Epilepsia* 59: 1062-71

Lupori L, Sagona G, Fuchs C, Mazziotti R, Stefanov A, et al. 2019. Site-specific abnormalities in the visual system of a mouse model of CDKL5 deficiency disorder. *Hum Mol Genet*

Marsh E, Fulp C, Gomez E, Nasrallah I, Minarcik J, et al. 2009. Targeted loss of Arx results in a developmental epilepsy mouse model and recapitulates the human phenotype in heterozygous females. *Brain* 132: 1563-76

Mazziotti R, Lupori L, Sagona G, Gennaro M, Della Sala G, et al. 2017. Searching for biomarkers of CDKL5 disorder: early-onset visual impairment in CDKL5 mutant mice. *Hum Mol Genet* 26: 2290-98

Melikishvili G, Epitashvili N, Tabatadze N, Chikvinidze G, Dulac O, et al. 2019. New insights in phenomenology and treatment of epilepsy in CDKL5 encephalopathy. *Epilepsy Behav* 94: 308-11

Moore YE, Kelley MR, Brandon NJ, Deeb TZ, Moss SJ. 2017. Seizing Control of KCC2: A New Therapeutic Target for Epilepsy. *Trends Neurosci* 40: 555-71

Muller A, Helbig I, Jansen C, Bast T, Guerrini R, et al. 2016. Retrospective evaluation of low long-term efficacy of antiepileptic drugs and ketogenic diet in 39 patients with CDKL5-related epilepsy. *Eur J Paediatr Neurol* 20: 147-51

Munoz IM, Morgan ME, Peltier J, Weiland F, Gregorczyk M, et al. 2018. Phosphoproteomic screening identifies physiological substrates of the CDKL5 kinase. *EMBO J* 37: pii: e99559.

Okuda K, Kobayashi S, Fukaya M, Watanabe A, Murakami T, et al. 2017. CDKL5 controls postsynaptic localization of GluN2B-containing NMDA receptors in the hippocampus and regulates seizure susceptibility. *Neurobiol Dis* 106: 158-70

Okuda K, Takao K, Watanabe A, Miyakawa T, Mizuguchi M, Tanaka T. 2018. Comprehensive behavioral analysis of the Cdkl5 knockout mice revealed significant enhancement in anxiety- and fear-related behaviors and impairment in both acquisition and long-term retention of spatial reference memory. *PLoS One* 13: e0196587

Olson HE, Demarest ST, Pestana-Knight EM, Swanson LC, Iqbal S, et al. 2019. Cyclin-Dependent Kinase-Like 5 Deficiency Disorder: Clinical Review. *Pediatr Neurol* 97: 18-25

Pizzo R, Gurgone A, Castroflorio E, Amendola E, Gross C, et al. 2016. Lack of Cdkl5 Disrupts the Organization of Excitatory and Inhibitory Synapses and Parvalbumin Interneurons in the Primary Visual Cortex. *Front Cell Neurosci* 10: 261

Price MG, Yoo JW, Burgess DL, Deng F, Hrachovy RA, et al. 2009. A triplet repeat expansion genetic mouse model of infantile spasms syndrome, Arx(GCG)10+7, with interneuronopathy, spasms in infancy, persistent seizures, and adult cognitive and behavioral impairment. *J Neurosci* 29: 8752-63

Puskarjov M, Kahle KT, Ruusuvuori E, Kaila K. 2014. Pharmacotherapeutic targeting of cation-chloride cotransporters in neonatal seizures. *Epilepsia* 55: 806-18

Ricciardi S, Ungaro F, Hambrock M, Rademacher N, Stefanelli G, et al. 2012. CDKL5 ensures excitatory synapse stability by reinforcing NGL-1-PSD95 interaction in the postsynaptic

compartment and is impaired in patient iPSC-derived neurons. *Nat. Cell Biol.* 14: 911-23

Rivera C, Voipio J, Payne JA, Ruusuvuori E, Lahtinen H, et al. 1999. The K+/Cl- co-transporter KCC2 renders GABA hyperpolarizing during neuronal maturation. *Nature* 397: 251-5

Rusconi L, Salvatoni L, Giudici L, Bertani I, Kilstrup-Nielsen C, et al. 2008. CDKL5 expression is modulated during neuronal development and its subcellular distribution is tightly regulated by the C-terminal tail. *J. Biol. Chem.* 283: 30101-11

Scala E, Ariani F, Mari F, Caselli R, Pescucci C, et al. 2005. CDKL5/STK9 is mutated in Rett syndrome variant with infantile spasms. *J.Med.Genet.* 42: 103-07

Scheffer IE, Berkovic S, Capovilla G, Connolly MB, French J, et al. 2017. ILAE classification of the epilepsies: Position paper of the ILAE Commission for Classification and Terminology. *Epilepsia* 58: 512-21

Symonds JD, Zuberi SM, Stewart K, McLellan A, O'Regan M, et al. 2019. Incidence and phenotypes of childhood-onset genetic epilepsies: a prospective population-based national cohort. *Brain* 142: 2303-18

Tang S, Wang IJ, Yue C, Takano H, Terzic B, et al. 2017. Loss of CDKL5 in Glutamatergic Neurons Disrupts Hippocampal Microcircuitry and Leads to Memory Impairment in Mice. *J Neurosci* 37: 7420-37

Tang X, Kim J, Zhou L, Wengert E, Zhang L, et al. 2016. KCC2 rescues functional deficits in human neurons derived from patients with Rett syndrome. *Proc Natl Acad Sci U S A* 113: 751-6

Wang IT, Allen M, Goffin D, Zhu X, Fairless AH, et al. 2012. Loss of CDKL5 disrupts kinome profile and event-related potentials leading to autistic-like phenotypes in mice. *Proc Natl Acad Sci U S A* 109: 21516-21

Weaving LS, Christodoulou J, Williamson SL, Friend KL, McKenzie OL, et al. 2004. Mutations of CDKL5 cause a severe neurodevelopmental disorder with infantile spasms and mental retardation. *Am.J.Hum.Genet.* 75: 1079-93

Yamada J, Okabe A, Toyoda H, Kilb W, Luhmann HJ, Fukuda A. 2004. Cl- uptake promoting depolarizing GABA actions in immature rat neocortical neurones is mediated by NKCC1. *J Physiol* 557: 829-41

Yennawar M, White RS, Jensen FE. 2019. AMPA receptor dysregulation and therapeutic interventions in a mouse model of CDKL5 Deficiency Disorder. *J Neurosci*: pii: 2041-18.

Zayachkivsky A, Lehmkuhle MJ, Fisher JH, Ekstrand JJ, Dudek FE. 2013. Recording EEG in immature rats with a novel miniature telemetry system. *J Neurophysiol* 109: 900-11

Zhu YC, Li D, Wang L, Lu B, Zheng J, et al. 2013. Palmitoylation-dependent CDKL5-PSD-95 interaction regulates synaptic targeting of CDKL5 and dendritic spine development. *Proc Natl Acad Sci U S A* 110: 9118-23

Figure 1 (Liao)

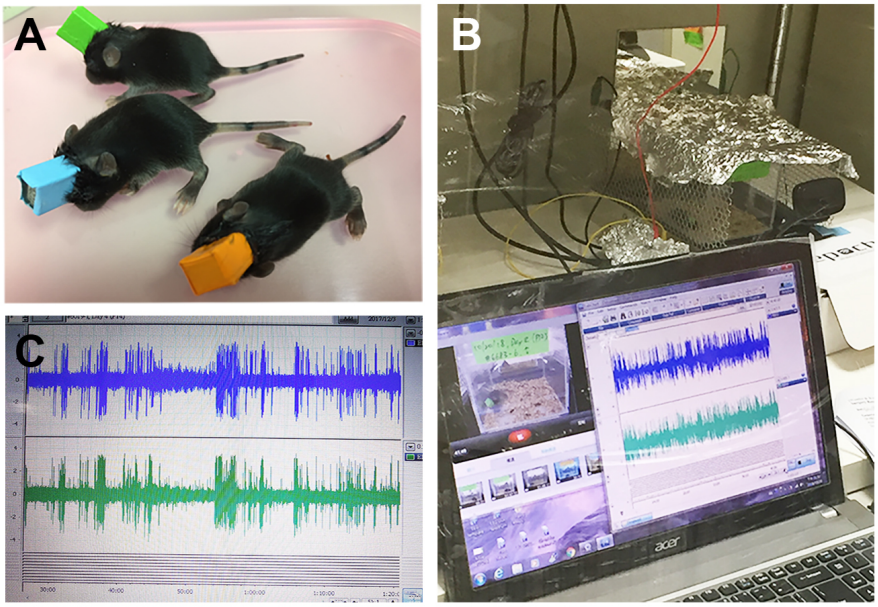

Figure 1. Wireless recordings of EEG from mouse pups. A transmitter including electrodes, a battery and an antenna in an epoxy-coated cube of 4 x 6 mm^3 in size was implanted in a mouse pup at postnatal day 10 (P10) of age (A). The implanted pup was placed in a transparent acrylic box on the top of the receiver and subjected to synchronized recording of EEG and behaviors (B). Seizure-like EEG activities were acquired in the sampling rate of 1000 Hz (C).

Figure 2 (Liao)

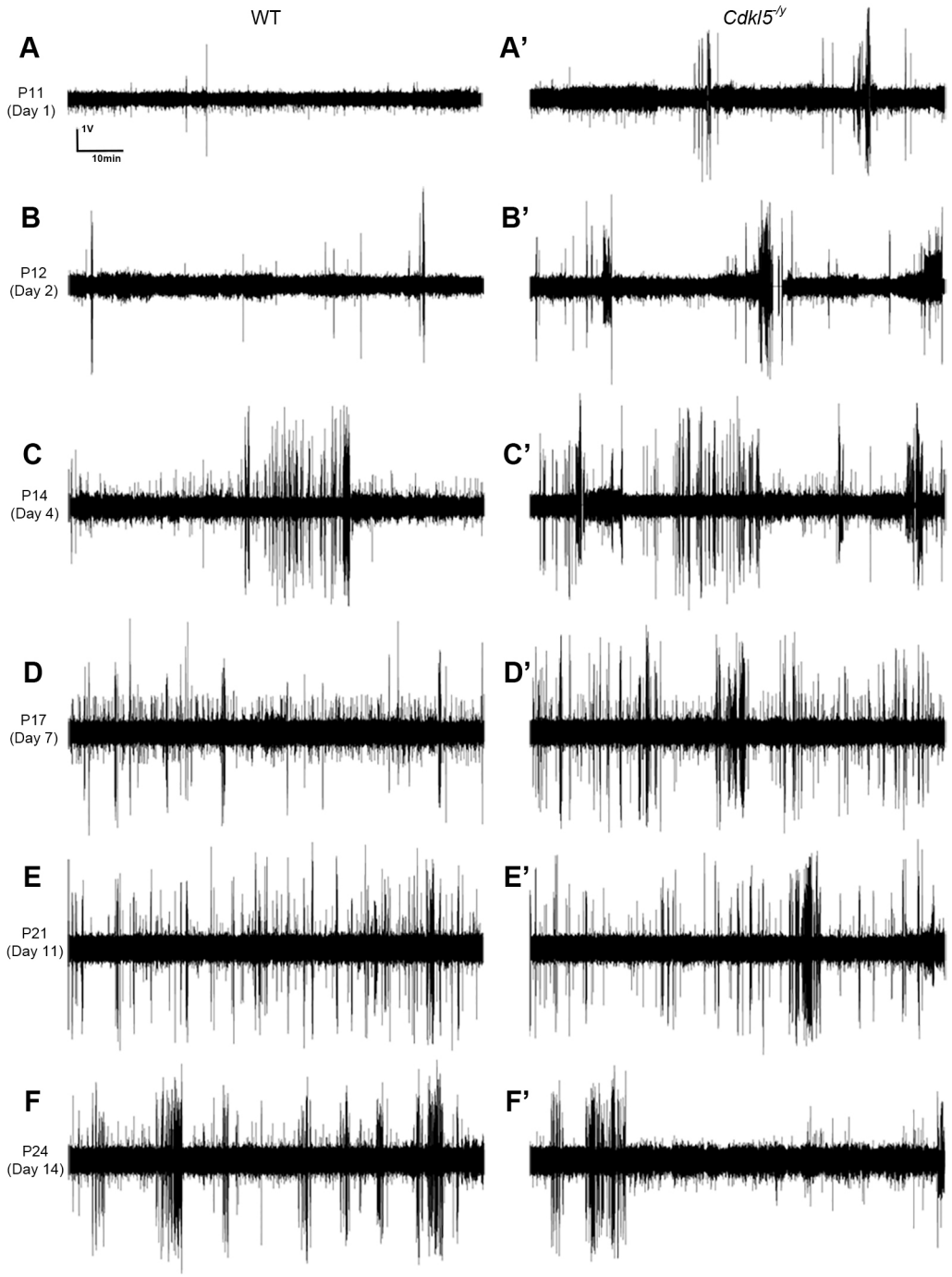

Figure 2. Longitudinal EEG activities in mouse pups. Representative EEG activities of a pairs of *Cdkl5*$^{-/y}$ and wild-type (WT) pups recorded for 100 minutes daily at P11, 12, 14, 17, 21, and 24. All the traces present the last 90 min (10 - 100 min). *Cdkl5*$^{-/y}$ pups (A'-F') display increased seizure-like discharges compared to WT pups (A-F) on the first three post-surgery days (A-C'); however, the number of bursts seems reduced in mutant compared to WT pup after weaning (P24, F and F').

Figure 3 (Liao)

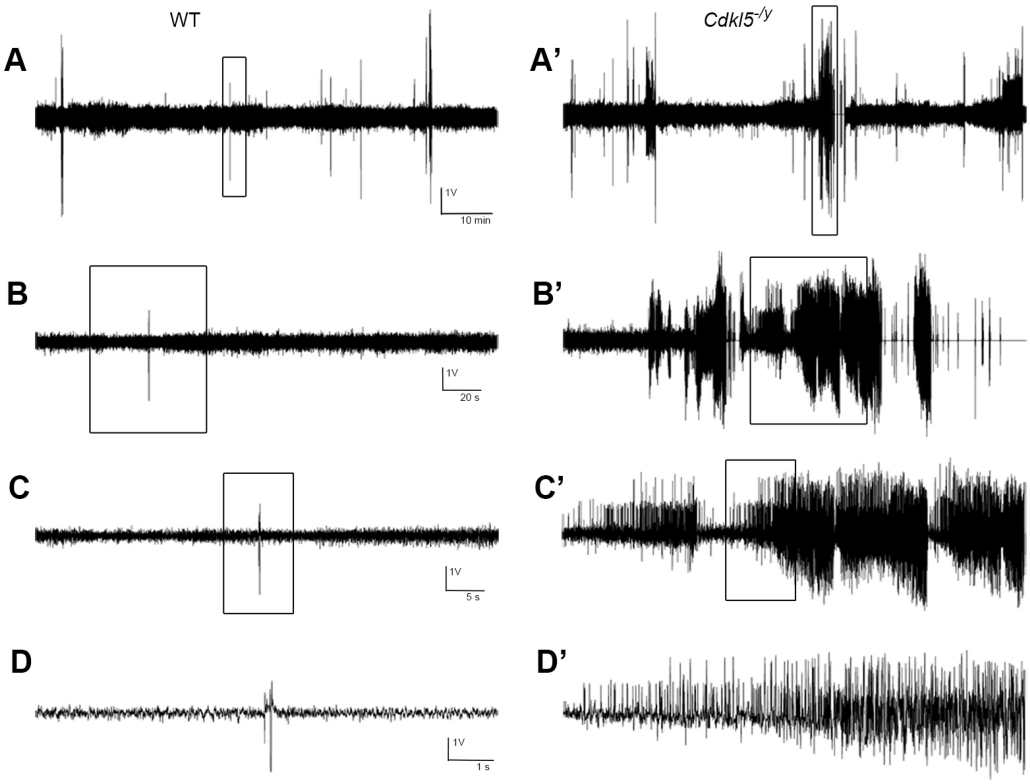

Figure 3. Seizure-like EEG activities in *Cdkl5*$^{-/y}$ pups at P12. Representative traces of EEG activities recorded from a pair of pups on the second day after implantation of transmitters. The whole trace in B (B') shows the boxed area (4 min) in A. The boxed areas in B (B', 60 sec) and C (C', 10 sec) are magnified as shown in C (C') and D (D'), respectively. Notably, the recurrent episodes of epileptiform discharges are manifested only in *Cdkl5*$^{-/y}$ pups (A'-D').

Figure 4 (Liao)

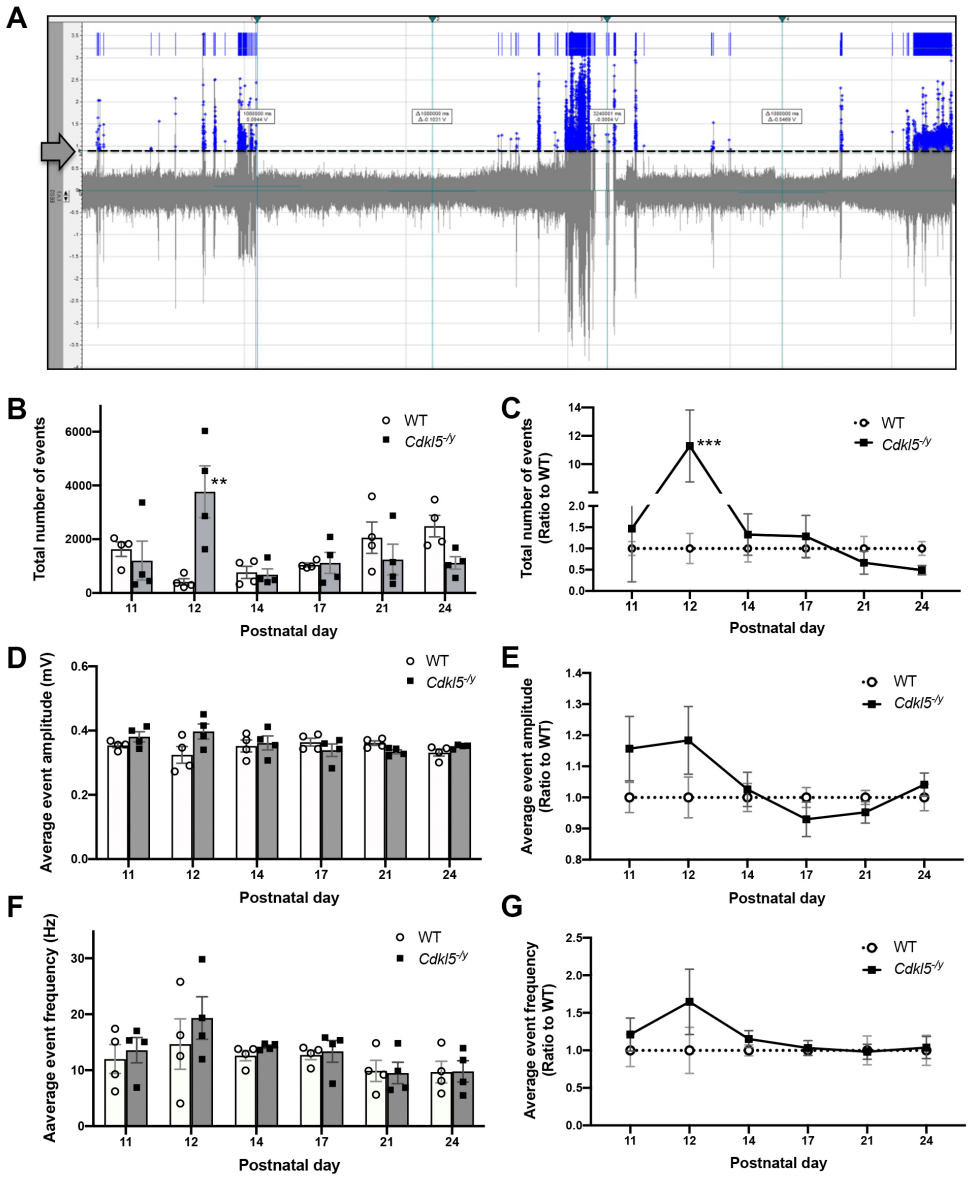

Figure 4. Increased number of events on EEG in *Cdkl5*$^{-/y}$ pups at P12. Population spike discharges with amplitudes higher than 0.9 volt (set as the threshold, equivalent to 0.225 mV of input amplitude) were defined as "events" using the pClamp10 software (arrow and dash line in A). The blue points and the vertical bars on the top indicate the detected events. The total number of events is significantly increased in pups at P12, which reach to ~12-fold compared to WT pups (B, C). Notably, *Cdkl5*$^{-/y}$ pups show slight age-dependent alterations in the event amplitude (D, E) and frequency (F, G), but the increases at P12 are not significant. All data are presented as mean ± SEM. ** $p < 0.01$; *** $p < 0.001$; mixed effects model followed by multiple comparison with Bonferroni's test.

Figure 5 (Liao)

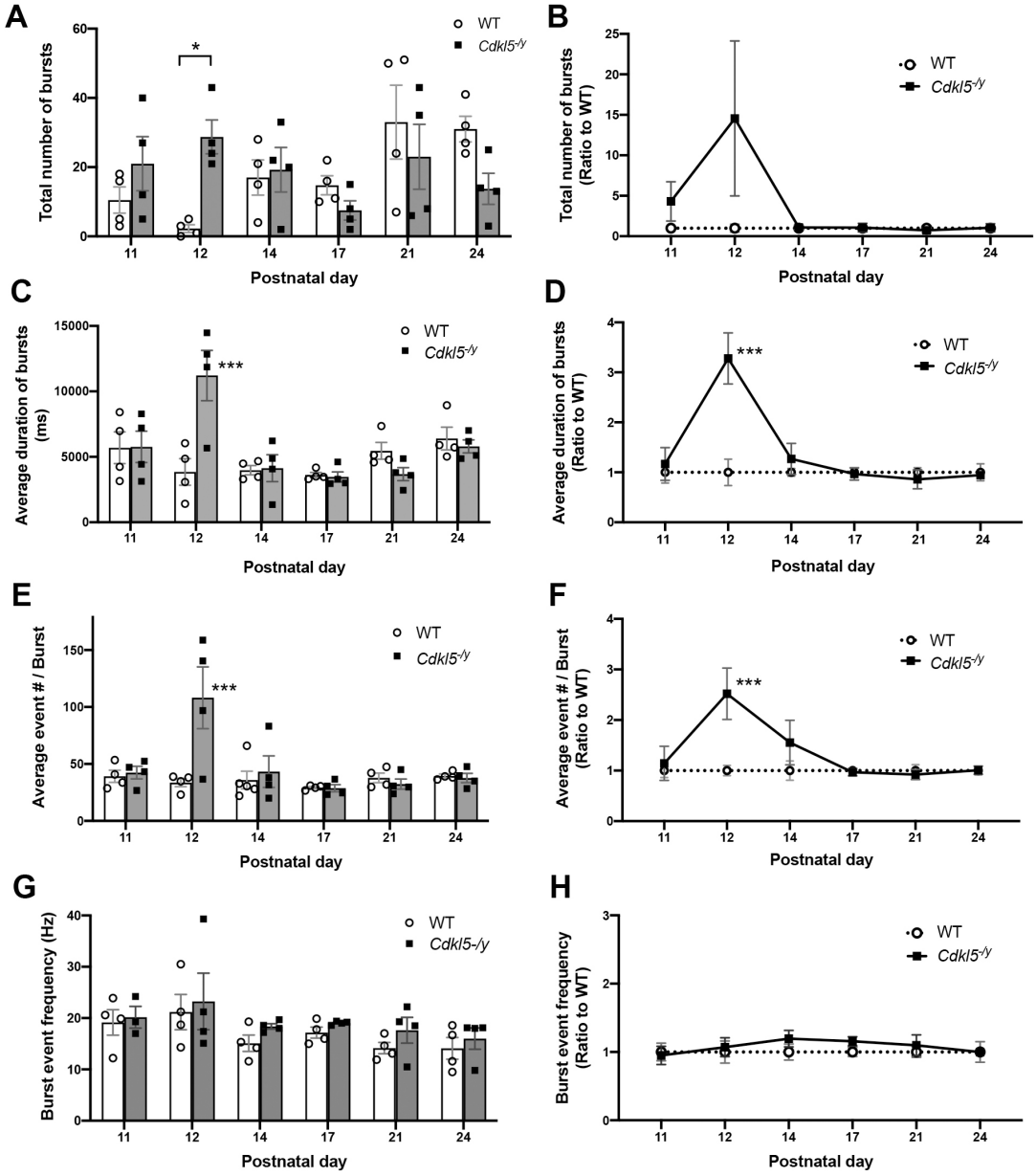

Figure 5. Increased burst activities on EEG in *Cdkl5*$^{-/y}$ pups at P12. A burst was defined as a series of continuous electrographic events for more than 20 events with the inter-event-interval for < 1 sec. *Cdkl5*$^{-/y}$ pups exhibit an increased total number of bursts (A, B), duration of bursts (C, D) and event number per burst (E, F) compared to WT littermate pups. The mean frequency of bursting events (G, H), however, is comparable between genotypes. All data are presented as mean ± SEM. * $p < 0.05$; *** $p < 0.001$; mixed effects model followed by multiple comparison with Bonferroni's test.

Figure 6 (Liao)

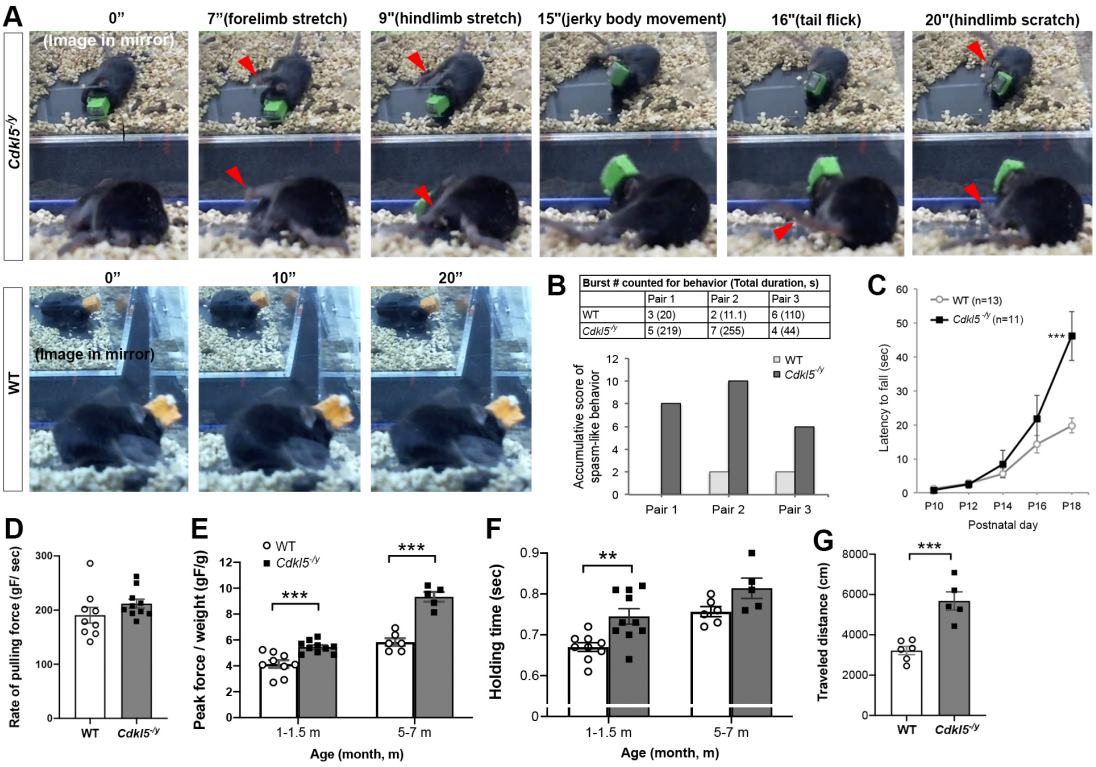

Figure 6. Spontaneous ictal behaviors in *Cdkl5*$^{-/y}$ pups and adults. Representative screenshots from videos of a bursting period show that *Cdkl5*$^{-/y}$ pups displayed continuous spasm-like movements within a prolonged burst of EEG activity (A, upper panel), while WT pups maintained the same posture throughout 20 sec of the burst (A, lower panel). The accumulative behavioral scores of spasm-like movements during the prolonged bursts are estimated in three pairs of *Cdkl5*$^{-/y}$ and WT pups (B). Notably, *Cdkl5*$^{-/y}$ pups developed ictal grasping in a wire suspension test, showing increased holding duration at the pre-weaning age of P18 (C). Moreover, *Cdkl5*$^{-/y}$ mice exhibited increased grip strength in peak force in both young adult (1-1.5 months) and middle age (5-7 months) under steady forces of pulling (D-F). The young adult *Cdkl5*$^{-/y}$ mice also showed increased holding time of grip (F). The longitudinal EEG recording during neonatal age does not attenuate the typical behavioral phenotype of hyperlocomotion in *Cdkl5*$^{-/y}$ mice in an open field test (G). All data are presented as mean ± SEM. ** $p < 0.01$; *** $p < 0.001$; Two-way repeated measures ANOVA followed by Bonferroni's test in C; Student's *t*-test in D-G.

Figure 7 (Liao)

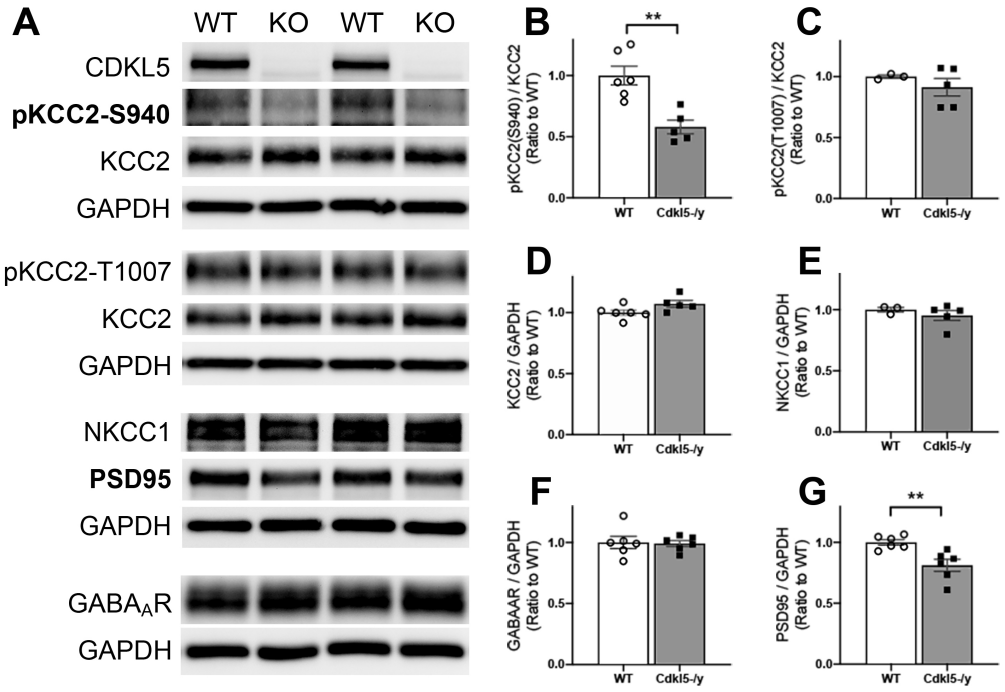

Figure 7. Reduced phosphorylation of KCC2 in the cortex of *Cdkl5*$^{-/y}$ pups at P12. Immunoblotting shows that loss of CDKL5 reduces the expression of phosphorylated KCC2 at serine 940 (pKCC2-S940; A, B) in the rostral cortex at P12. No significant alteration is found in protein expression of total KCC2, phosphorylated KCC2 at threonine 1007 (pKCC2-T1007), NKCC1 and GABA$_A$ receptor. Quantification of protein expression was performed by Image J with GAPDH as a loading control. Data are derived from three litters and presented as mean ± SEM. ** $p < 0.01$, Student's *t*-test.